Insulin Amyloid Fibrils Form an Inclusion Complex with Molecular Iodine: A Misfolded Protein as a Nanoscale Scaffold†

Wojciech Dzwolak*

Institute of High Pressure Physics, Polish Academy of Sciences, Sokolowska 29/37, 01-142 Warsaw, Poland, and Department of Chemistry, Warsaw University, Pasteura 1, 02-093 Warsaw, Poland

Received September 23, 2006; Revised Manuscript Received December 8, 2006

ABSTRACT: The study describes formation of an intensely violet inclusion complex of insulin amyloid fibrils and molecular iodine. Resonance Raman spectra of complexes formed by staining mature insulin fibrils with iodine and by seeding fibrils in the presence of iodine imply similar topologies of entrapped iodine and oligoiodide species. Iodine captured by growing fibrils remains accessible to a bulk chemical reagent. In light of its small size and the fact that iodine can partition into polar as well as nonpolar media, the data suggest that intrafibrillar structure of insulin amyloid is densely packed with no appreciable void volumes capable of accommodating iodine atoms. The complex is stable: only drastic perturbation of the β-pleated fibrous scaffold by dimethyl sulfoxide (rather than of the β-sheet conformation) leads to the release of iodine atoms from surface moieties. While the reaction between iodine and in vivo amyloid deposits was first described by Virchow in the 19th Century [Virchow, R. (1854) *Virchows Arch. 6*, 268−271], the underlying molecular mechanism has not been thoroughly explored since then. This work shows how the long-forgotten concept can be utilized as a probe of void volumes in protein fibrils, providing a new tool for structural studies on amyloids, and a model for design of protein-based drug delivery media.

Non-native β-sheet-rich protein fibrils, the so-called amyloids, have been implicated in several degenerative conditions, such as Alzheimer's disease or the prion-associated Creutzfeldt-Jakob disease. By now, more than 20 human disorders have been linked to in vivo amyloid deposits (*1*−*3*). Historically, the first probe of histological amyloid deposits was the iodine staining assay described by Virchow in the mid-19th Century (*4*, *5*). Because it was reminiscent of the starch−iodine reaction, the effect was errantly attributed to the presence of a "carbohydrate moiety", and the term "amyloid" was coined (*6*, *7*). Ironically, after more than 150 years since these pioneering works, molecular mechanisms underlying the iodine reaction remain unknown. By analogy to the blue iodine−starch complex, which has been linked to linear polyiodides trapped within amylose coil (*8*−*10*), it could be suggested that a similar scenario underlies the iodine−amyloid reaction. In this work, Virchow's findings are revisited using insulin fibrils as a model amyloid. It is demonstrated that iodine is not trapped within solvent-protected cavities but is docking only at external solvent-accessible surfaces of the fibrils. This holds true even when insulin fibrils form gradually in the presence of iodine, which is thus enabled to penetrate the fibrils' internal cavities. Given the compactness of iodine and polyiodide species and solubility in polar as well as nonpolar solvents, it appears unlikely that the insulin fibrils possess any appreciable void volumes capable of entrapping the stain. It is argued that the same approach may prove very insightful in studying protein fibrillation in the context of void volumes and volume fluctuations.

While detailed structural studies on amyloid void volumes are scarce, such knowledge is urgently needed for a comprehensive thermodynamic description of amyloidogenic stacking of proteins (*11*, *12*), as well as a guide to possible applications of protein fibrils, e.g., as drug delivery media. For certain amyloid specimens, the presence of a spacious central canal was implied by local high-resolution probes, such as cryoelectron microscopy (*13*). An idea that amyloids are nanotubes filled with water has been adopted by Perutz et al. (*14*). Although our recent FT-IR[1] study showed no evidence of water trapped within insulin fibrils (*15*), this does not imply a lack of cavities, which may exist while remaining "dry". Namely, water filling a tiny and nonpolar cavity would be significantly frustrated in terms of unsaturated hydrogen bonding and therefore thermodynamically disfavored. In this context, the fundamental advantage of iodine: the small size and avid partitioning into both polar and nonpolar environments become apparent. Unlike iodine, several organic compounds, such as Congo Red or thioflavin T, have become routine means of staining amyloid fibrils (*16*−*19*). However, a number of important structural problems related to protein fibrils can be addressed exclusively (or more adequately) by using the iodine probe.

† Financial support from the Polish Ministry of Education and Science, Grant 2P04A 011 28 (2005−2007), is gratefully acknowledged.

* To whom correspondence should be addressed. Phone: +48 22 888 0237. Fax: +48 22 632 4218. E-mail: wdzwolak@unipress.waw.pl.

[1] Abbreviations: AFM, atomic force microscopy; DMSO, dimethyl sulfoxide; EtOD, deuterated ethanol; FT-IR, Fourier transform infrared; ThT, thioflavin T.

10.1021/bi061985l CCC: $37.00
Published on Web 01/20/2007

MATERIALS AND METHODS

Samples and Seeding. Bovine insulin (1 wt %, from Sigma) in 100 mM NaCl and D_2O (pD 1.8) was seeded with sonicated preformed insulin fibrils at a 100:1 protein weight ratio. Samples were incubated in the presence of 0.4 mM I_2 and 3 mM KI. A single sample preparation was used for simultaneous acquisitions of time-resolved UV and FT-IR spectra at 37 °C. As noted above, the protein was dissolved in heavy water to permit observation of the conformation-sensitive amide I band (between 1600 and 1700 cm^{-1}) (*15*). Other details concerning FT-IR were as described previously (*15*). After fibrillation was complete, amyloid samples were assayed for AFM imaging, after approximately 500-fold dilution with water and brief sonication; other details were described previously (*20*) or are specified in the figure legends.

Resonance Raman Spectroscopy. Samples of the insulin fibril−I_2 complex were subjected to Raman measurements on a Jobin Yvon-Spex T64000 Raman spectrometer equipped with a Kaiser holographic notch filter, an 1800 grooves/mm holographic grating, and a 1024 × 256 pixel nitrogen-cooled charge-coupled device detector. Raman scattering was excited with the 514.5 nm argon laser line.

Titration with Ascorbic Acid and Control Experiments. Ascorbic acid (2.66 mM) in water (pH 6) was used for titration of the amyloid−iodine complexes. The titration was carried out at 25 °C. Small (1 μL) portions of the ascorbic acid solution were gradually added to a vigorously stirred complex sample. The following redox reaction was very fast and complete with no residual intensity left.

RESULTS AND DISCUSSION

Figure 1A shows stacked time-resolved UV absorption difference spectra of bovine insulin doped with iodine and undergoing gradual fibrillation upon seeding with preformed amyloid templates. The UV and FT-IR (inset, Figure 1A) spectra were collected simultaneously for the same protein preparation and under identical conditions. The spectral changes in the amide I′ band reflect ongoing refolding of native α-helices absorbing at 1654 cm^{-1} into stacked β-strands at 1625 cm^{-1}, which constitute the fundamental secondary structural motif of amyloid fibrils (*15*). These changes are accompanied by the sample changing color from yellow to violet, which in the UV spectra is manifested in the appearance of the band around 495 nm. The intensive violet color is the first tangible aspect of the formation of the inclusion complex between the fibrils and iodine. Interestingly, this straightforward effect was not observed in an earlier study on staining of in vitro-grown insulin fibrils with iodine (*21*). The inclusion complex is formed also at neutral pH (pD). The acidic conditions used in this study reflect only the peculiar requirements of insulin in forming fibrils. The kinetic curves in Figure 1B reflect simultaneous stacking of the β-pleated conformations and the formation of the complex. The latter process is apparently accelerated in the final stages of fibrillation (the curves split, Figure 1B), namely, when the lateral wall-to-wall association of protofilaments prevails (*20*). This is an early indication that iodine-trapping moieties of insulin fibrils are placed on their surfaces, as opposed to being buried in the amyloid interior.

The conditions of fibrils' elongation (an excess of iodide ions and high ionic strength) were adjusted so that the oxidative activity of molecular iodine remained low and no side chemical reactions took place. In fact, whether iodine modifies the protein covalently or affects its misfolding−fibrillation pathways is a very important issue that must be addressed when employing molecular iodine as a stain. Any chemical modification of a protein by iodine is a redox process and as such is strongly dependent on reduction potential of the I_2/I^- pair. The diluted 0.4 mM I_2 in the almost 10-fold molar excess of iodide anions and at a high (100 mM NaCl) ionic strength does not react appreciably with fibrillating insulin. A very simple way of verifying that is titration of the amyloid−iodine complex with ascorbic acid and comparing the outcome with an analogous control titration of iodine solution in the absence of protein. Should a side chemical reaction between iodine and insulin take place, this would inevitably lead to a decrease in the total amount of I_2, and thus to a corresponding decrease of the amount of ascorbic acid needed for the complete titration. Under the specific conditions of this study, this was not observed, however. Further proof that the conditions used in this study do not perturb the fibrillation process came from

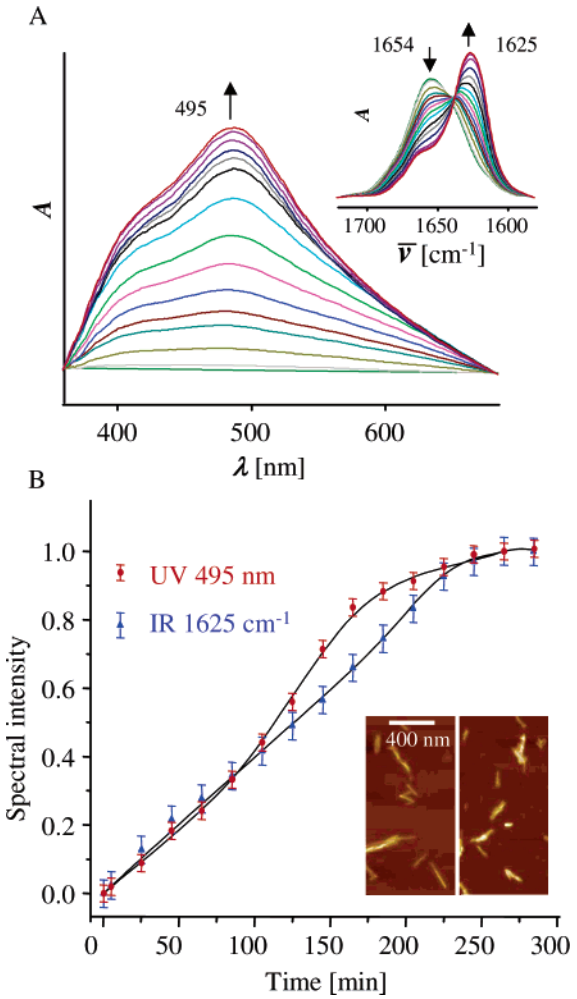

FIGURE 1: (A) Time-dependent difference UV absorption spectra of bovine insulin seeded at 37 °C, in the presence of iodine. The inset shows FT-IR spectra collected simultaneously for an identical sample and under identical conditions. (B) Normalized time dependencies of the spectral components assigned to the β-sheet and to the iodine−amyloid complex. The AFM images of the mature I_2−amyloid complex feature typical fibrous morphologies (inset).

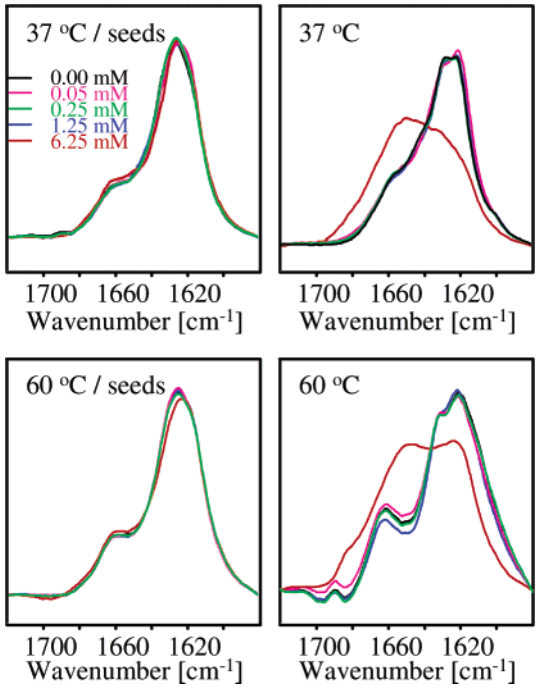

FIGURE 2: Influence of increasing concentrations of iodine on insulin fibrillation. Normalized and solvent-subtracted FT-IR spectra of insulin fibrils (the amide I band) formed through a 48 h incubation of 1 wt % insulin in 100 mM NaCl and 15 wt % EtOD in D_2O (pD 1.8) at 60 °C, or through intensive vortexing at 1400 rpm and 37 °C. The fibrillation routines were carried out in the presence or absence of 1 wt % sonicated preformed fibrils (seeds). Concentrations of iodine were in the range from 0 to 6.25 mM and are indicated by the color of the corresponding line.

the similarity of kinetics of the seed-induced fibrillation in the presence and absence of iodine: the practical identity of the infrared spectra, the thioflavin T fluorescence, and AFM images of amyloid fibrils grown in the presence and absence of diluted iodine (inset of Figure 1B). Although insulin, which lacks methionine or reduced cysteine residues, is not expected to be easily oxidized by iodine under the conditions of this study, it may still undergo a covalent modification at the sites of its four tyrosine residues. In fact, it was noticed that an excessive amount of iodine does perturb or even prevent insulin aggregation. This problem is signalized in Figure 2, showing FT-IR spectra of several amyloid preparations formed at an increasing concentration of iodine. In these control experiments, potassium iodide was replaced with diluted ethanol as a "solubilizer" of iodine, since the concentrated salt tends to salt out the native protein, thus affecting the fibrillation per se. The aggregation routines have been carried out either at 60 °C in unstirred protein samples or at 37 °C and with intensive vortexing. In addition, the influence of preformed amyloid seeds was examined. According to the spectra presented in Figure 2, the presence of iodine does sway the fibrillation process only at the highest concentration that was examined (6.25 mM), and in the absence of preformed amyloid templates (37 and 60 °C), i.e., when the fibrillation is very slow and preceded by a long lag phase of spontaneous formation of aggregation nuclei (*15*, *20*). The difference in iodine reactivity toward the seeded and unseeded samples can be explained in terms of prolonged denaturation and simultaneous exposure of tyrosine residues to the bulk solvent (and iodine) taking place in unseeded samples. The fibrillation occurs much faster when they are seeded, which effectively prevents undesirable lateral processes. It appears, therefore, that at least for a "methionine-free" proteins, like insulin, it is rather easy to establish a set of appropriate experimental conditions by (i) diluting iodine, (ii) adding an excess of iodide ions to reduce the oxidative strength and chemical reactivity of the stain, and (iii) carrying out fibrillation in the presence of seeds.

The insulin amyloid−iodine complex, once formed, is stable; e.g., up to 90 °C, no thermochromism typical for the starch−iodine adduct is observed (data not shown). This coincides with the marked thermal stability of the insulin amyloid itself (*15*). The extinction coefficient at 495 nm can be roughly estimated to be 4000 $dm^3\ cm^{-1}\ (mol\ of\ I_2)^{-1}$ in an excess of amyloid. This value, along with the strong light scattering properties of the insoluble fibrils, determines a limit of detection of I_2 molecules trapped by the fibrils. It can thus be estimated that fewer than one I_2 molecule per 120 insulin monomers (forming fibrils) would be undetectable under the experimental conditions of this study. It must be stressed, however, that establishing the stoichiometry of the complex, i.e., the number of iodine-specific binding sites per insulin monomer, appears to pose a significantly more difficult task. Namely, the increasing concentration of iodine leads to dramatic precipitation of the iodine−fibril complex. Moreover, the high iodine content increases the risk of undesirable side processes that could lead to chemical modifications of fibrils. Finally, given the structural complexity and polymorphism of insulin fibrils (*20*, *22*), it is necessary to show convincingly first whether there is just one or more types of I_2-binding sites. These circumstances, along with the difficulty to control nanodispersion of insoluble protein fibrils, make the task of calculating the binding constant quite challenging. This is particularly complicated by the fact that, as Raman resonance data will show, a single molecular identity cannot be convincingly assigned to the amyloid-bound iodine.

The conditions of growth of insulin fibrils chosen in this study allow iodine to be encapsulated within central solvent-protected cavities *in statu nascendi* of the amyloid. Should there be accessible internal void volumes, at least a portion of iodine would be trapped within it, as proposed for starch (*8*). As a result, the binding may occur according to distinct scenarios when iodine is added to already grown mature fibrils (growth completed and void volumes closed), and when iodine is present throughout the elongation phase (accessible void volumes). Resonance Raman spectra of the inclusion complexes with iodine formed after and during elongation of insulin fibrils are compared in Figure 3. While the spectra share a number of features with the Raman data obtained for other inclusion complexes of iodine with amylose (*8*, *23*, *24*), xylan (*25*), or polyvinyl alcohol (*23*, *26*, *27*), several bands are reminiscent of the Raman resonance spectra of molecular iodine in liquid (*28*, *29*) and vapor (*30*) phases. It seems reasonable to propose that the main reason for the complexity of the observed resonance Raman bands is the presence of distinct iodine forms (I_2 and oligoiodides) being entrapped by the fibrils, and giving rise to fundamental bands, as well as overtones and combination bands (*27*). The band at 152 cm^{-1} is visible only in samples formed by mixing mature fibrils with an iodine solution (Figure 3). The band has been assigned to I_5^- stretching (*26*), which, as a thermodynamically more stable bent C_{2V} form

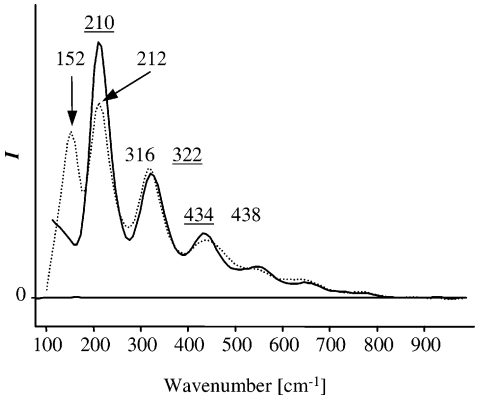

FIGURE 3: Resonance Raman spectra of iodine−fibril complexes formed upon fibrillation of insulin in the presence of iodine (—, underlined numbers) and through staining fibrils already grown with iodine (···). The virtually flat black lines at the bottom correspond to control experiments with unmixed iodine and insulin fibril samples.

(*31*), is likely to receive additional stabilization upon intercalating into fibrils' β-sheets. The topological complexity of amyloid fibrils provides moieties capable of stabilization and entrapment of different oligoiodide species. A swift transition of such an oligo- or polyiodide anion into (under the topological constraints determined by the fibrils' structure) a more thermodynamically stable form can be coupled to elasticity of the fibrous scaffold, especially during its growth. As far as the resonance Raman spectra are concerned, either type of complex preparation is kinetically stable. This, however, does not mean thermodynamic equivalence.

Iodine buried in intrafibrillar clefts would be effectively sequestered from bulk solution and thus "unavailable" as a chemical reactant. A very simple experiment addressing this problem in presented in Figure 4. The violet, iodine-stained fibrils grown during the experiment described in Figure 1 were treated with diluted L-ascorbic acid (vitamin C). While ascorbic acid does not affect the stability and morphology of the insulin fibrils, it reduces iodine to iodide ions immediately, which results in the simultaneous disappearance of the violet color. The ensuing spectra show how a gradual titration of the inclusion complex with ascorbic acid causes an immediate disappearance of the 495 nm absorption band from the corresponding UV spectrum (Figure 4A). The limit of detection of iodine trapped by the fibrils, which has been estimated at a single I_2 molecule per 120 insulin monomers, is sufficient to rule out buried continuous polyiodine/polyiodide chains running alongside the fibril axis. This is simple yet convincing proof that practically all iodine atoms "swallowed" by the elongating amyloid fibrils remain located on the external and easily accessible (to ascorbic acid) surfaces of the fibrils. As expected, the same result is obtained, when the complex is formed by mixing iodine with mature fibrils. Given the particular conditions, under which the complex was formed, the result casts doubt on whether there are any void volumes in the structure of the fibril capable of trapping iodine. While this finding challenges certain structural models of amyloid fibrils (e.g., refs *13*, *14*, and *32*), at the same time it remains in accordance with the recent FT-IR study on cavities in insulin amyloid fibrils (*15*).

To further characterize the molecular environment hosting iodine on insulin fibrils' surfaces, it was useful to compare

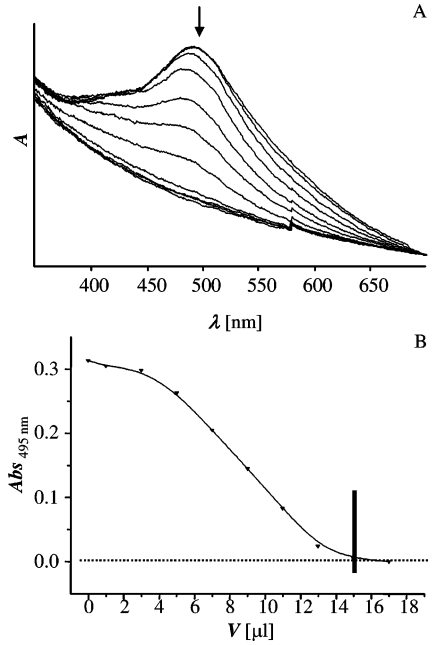

FIGURE 4: (A) UV spectra-monitored titration of iodine trapped upon fibrils' growth with ascorbic acid. (B) Quantitative plot showing that titration is complete with no residual spectral intensity corresponding to buried and unreacted iodine.

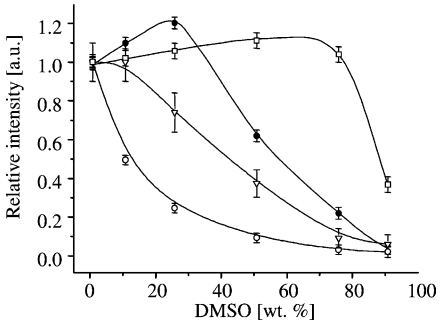

FIGURE 5: Insulin fibrils dissolved in DMSO, probed by ThT fluorescence [λ_{excit} = 450 nm, and λ_{em} = 482 nm (○)], light scattering at 350 nm (●), the intensity of the β-sheet IR component at 1625 cm^{-1} (□), and UV absorption of the iodine−amyloid complex at 495 nm (▽). Each titration was carried out at 25 °C, at the identical DMSO (as specified by the coordinates) and protein (0.3 wt %) concentrations.

how a gradual perturbation of the fibrous topology affects the iodine complex absorption juxtaposed with a range of different optical "probes". Because such a perturbation must not enhance any secondary chemical reaction, an appropriate set of conditions was sought. Titration with dimethyl sulfoxide (DMSO), known to disintegrate amyloids (*33*), has been chosen. Figure 5 shows how a high concentration of DMSO leads to a gradual decay of the specific fibril fluorescence of thioflavin T followed by decreasing light scattering, and β-sheet content. Overlaid is the curve corresponding to the falling absorption of the iodine complex at 495 nm. The complex appears to disintegrate simultaneously with decreasing fluorescence and light scattering rather than unfolding of the β-sheet structure. This hints at the possible role played by tertiary contacts and side chain interactions in providing a stable "nest" for the oligoiodine chains (*8*, *9*).

In conclusion, the novel application of iodine, the old-fashioned amyloid probe, implies the absence of cavities in insulin fibrils. The iodine-assisted growth of amyloid fibrils was followed by the test of topological accessibility of "trapped" iodine with ascorbic acid. This approach provides a simple, universal means of addressing the problem of void volumes in amyloid fibrils. A remarkable advantage of this approach, when combined with resonance Raman spectroscopy, lies in its sensitivity to the local topology and environment of iodine-binding sites. Deconvolution of the Raman bands of amyloid-trapped I_2 and oligoiodide species may provide a unique biophysical tool of physicochemical characterization of surfaces of amyloid fibrils. That could shed light on the molecular basis of their varying "strain-dependent" biological activity.

ACKNOWLEDGMENT

I am grateful to Prof. Roland Winter and Mr. Vytautas Smirnovas (Dortmund University, Dortmund, Germany) for AFM measurements and to Prof. Jolanta Bukowska and Dr. Andrzej Kudelski (Warsaw University) for resonance Raman measurements.

SUPPORTING INFORMATION AVAILABLE

FT-IR spectra of the iodine−amyloid complex titrated with DMSO. This material is available free of charge via the Internet at http://pubs.acs.org.

REFERENCES

1. Uversky, V. N., and Fink, A. L. (2004) Conformational constraints for amyloid fibrillation: The importance of being unfolded, *Biochim. Biophys. Acta 1698*, 131−153.
2. Ross, C. A., and Poirier, M. A. (2004) Protein aggregation and neurodegenerative disease, *Nat. Med. Suppl.*, S10−S17.
3. Dobson, C. M. (2003) Protein folding and misfolding, *Nature 426*, 884−890.
4. Virchow, R. (1853) Nouvelles observations sur la substance animale analogue à la cellulose végétale, *C. R. Acad. Sci., Paris 37*, 860−861.
5. Virchow, R. (1854) Weitere Mittheilungen über das Vorkommen der pflanzlichen Cellulose beim Menschen, *Virchows Arch. 6*, 268−271.
6. Aterman, K. (1976) A historical note on the iodine-sulphuric acid reaction of amyloid, *Histochemistry 49*, 131−143.
7. Puchtler, H., and Sweat, F. J. (1966) A review of early concepts of amyloid in context with contemporary chemical literature from 1839 to 1859, *Histochem. Cytochem. 14*, 123−134.
8. Teitelbaum, R. C., Ruby, S. L., and Marks, T. J. (1978) On the structure of starch-iodine, *J. Am. Chem. Soc. 100*, 3215−3217.
9. Calabrese, V. T., and Khan, A. (2000) Polyiodine and polyiodide species in an aqueous solution of iodine + KI: Theoretical and experimental studies, *J. Phys. Chem. A 104*, 1287−1292.
10. Svensson, P. H., and Kloo, L. (2003) Synthesis, structure, and bonding in polyiodide and metal iodide-iodine systems, *Chem. Rev. 103*, 1649−1684.
11. Foguel, D., Suarez, M. C., Ferrao-Gonzales, A. D., Porto, T. C. R., Palmieri, L., Einsiedler, C. M., Andrade, L. R., Lashuel, H. A., Lansbury, P. T., Kelly, J. W., and Silva, J. L. (2003) Dissociation of amyloid fibrils of α-synuclein and transthyretin by pressure reveals their reversible nature and the formation of water-excluded cavities, *Proc. Natl. Acad. Sci. U.S.A. 100*, 9831−9836.
12. Smirnovas, V., Winter, R., Funck, T., and Dzwolak, W. (2006) Protein amyloidogenesis in the context of volume fluctuations: An insulin case study, *Chem. Phys. Chem. 7*, 1046−1049.
13. Jimenez, J. L., Guijarro, J. L., Orlova, E., Zurdo, J., Dobson, C. M., Sunde, M., and Saibil, H. R. (1999) Cryo-electron microscopy structure of an SH3 amyloid fibril and model of the molecular packing, *EMBO J. 18*, 815−821.
14. Perutz, M. F., Finch, J. T., Berriman, J., and Lesk, A. (2002) Amyloid fibers are water-filled nanotubes, *Proc. Natl. Acad. Sci. U.S.A. 99*, 5591−5595.
15. Dzwolak, W., Loksztejn, A., and Smirnovas, V. (2006) New insights into the self-assembly of insulin amyloid fibrils: An H-D exchange FT-IR study, *Biochemistry 45*, 8143−8151.
16. Naiki, H., Higuchi, K., Hosokawa, M., and Takeda, T. (1989) Fluorometric determination of amyloid fibrils in vitro using the fluorescent dye, thioflavin T1, *Anal. Biochem. 177*, 244−249.
17. LeVine, H. (1999) Quantification of β-sheet amyloid fibril structures with thioflavin T, *Methods Enzymol. 309*, 274−284.
18. Bennhold, H. (1922) Eine spesifische Amyloid-farbung mit Kongrot, *Munchen. Med. Wochen. 69*, 1537−1538.
19. Nilsson, K. P. R., Herland, A., Hammarstrom, P., and Inganas, O. (2005) Conjugated polyelectrolytes: Conformation-sensitive optical probes for detection of amyloid fibril formation, *Biochemistry 44*, 3718−3724.
20. Jansen, R., Dzwolak, W., and Winter, R. (2005) Amyloidogenic self-assembly of insulin aggregates probed by high resolution atomic force microscopy, *Biophys. J. 88*, 1344−1353.
21. Cooper, J. H. (1974) Selective amyloid staining as a function of amyloid composition and structure. Histochemical analysis of the alkaline Congo red, standardized toluidine blue, and iodine methods, *Lab. Invest. 31*, 232−238.
22. Dzwolak, W., Smirnovas, V., Jansen, R., and Winter, R. (2004) Insulin forms amyloid in a strain-dependent manner: An FT-IR spectroscopic study, *Protein Sci. 13*, 1927−1932.
23. Heyde, M. E., Rimai, L., Kilponen, R. G., and Gill, D. (1972) Resonance-enhanced Raman spectra of iodine complexes with amylose and poly(vinyl alcohol), and of some iodine-containing trihalides, *J. Am. Chem. Soc. 94*, 5222−5227.
24. Teitelbaum, R. C., Ruby, S. L., and Marks, T. J. (1980) A resonance Raman/iodine Moessbauer investigation of the starch-iodine structure. Aqueous solution and iodine vapor preparations, *J. Am. Chem. Soc. 102*, 3322−3328.
25. Yu, X., and Atalla, R. H. (2005) The complex of xylan and iodine: The induction and detection of nanoscale order, *Carbohydr. Res. 340*, 981−988.
26. Sengupta, A., Quitevis, E. L., and Holtz, M. W. (1997) Effect of high pressure on vibrational modes of polyiodides in poly(vinyl alcohol) films, *J. Phys. Chem. B 101*, 11092−11098.
27. Sengupta, A., Holtz, M., and Quitevis, E. L. (1996) Temperature-dependent resonance Raman study of iodine-doped poly(vinyl alcohol) films, *Chem. Phys. Lett. 263*, 25−32.
28. Kiefer, W., and Bernstein, H. J. (1973) Resonance Raman spectroscopic study on iodine in various organic solvents: Spectroscopic constants and halfband widths of the I_2 vibration, *J. Raman Spectrosc. 1*, 417−431.
29. Matsuzaki, S., and Maeda, S. (1974) An excitation profile study of the resonance Raman effect of I_2 in solutions, *Chem. Phys. Lett. 28*, 27−30.
30. Rousseau, D. L. (1976) Resonance Raman scattering of light from a diatomic molecule, *J. Chem. Phys. 64*, 3519−3537.
31. Sharp, S. B., and Gellene, G. I. (1997) Ab initio calculations of the ground electronic states of polyiodide anions, *J. Phys. Chem. A 101*, 2192−2197.
32. Jimenez, J. L., Nettleton, E. J., Bouchard, M., Robinson, C. V., Dobson, C. M., and Saibil, H. R. (2002) The protofilament structure of insulin amyloid fibrils, *Proc. Natl. Acad. Sci. U.S.A. 99*, 9196−9201.
33. Hirota-Nakaoka, N., Hasegawa, K., Naiki, H., and Goto, Y. (2003) Dissolution of β_2-microglobulin amyloid fibrils by dimethylsulfoxide, *J. Biochem. 134*, 159−164.

BI061985L